A geomagnetic field model incorporating Earth's mantle conductivity

Hongbo Yao and Keke Zhang
Macau Institute of Space Technology and Application, Taipa, Macao, China
Email: hongbo.yao@outlook.com

Swarm 10 Year Anniversary & Science Conference 2024

Sources of near-Earth magnetic Field

- **<u>Magnetic measurements:</u>**
  - Core dynamics
  - Lithospheric magnetization
  - Ocean circulation and tides
  - Ionospheric currents and electromagnetic (EM) induction in the Earth
  - Magnetospheric currents and EM induction
  - Ionosphere-magnetosphere coupling currents

- **<u>Magnetic field models:</u>**
  - Separate different sources by geomagnetic field modeling
  - Those rapidly time-varying magnetospheric primary and Earth induced fields play important role in high-resolution geomagnetic field modeling

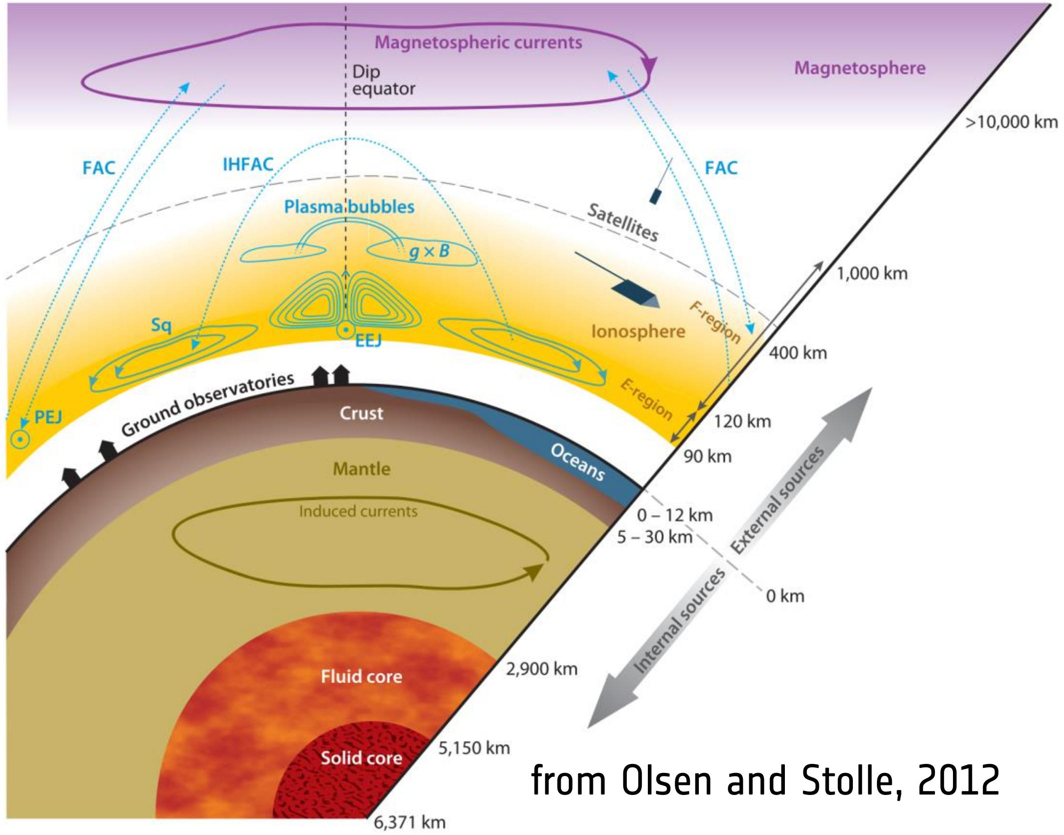

from Olsen and Stolle, 2012

Sources of near-Earth magnetic Field

Motivation

How does CM and CHAOS models deal with magnetospheric primary and induced fields?

- Spatial: by spherical harmonic (SH) expansion
- **Temporal:**
  - **CM model series (CM5, CM6)**: by a series of 1-hour time bins
    - EM induction equations are not invoked
    - Many parameters are needed (in CM6, magnetosphere/total = 685110/734670≈93%)
  - **CHAOS model series**: by a linear function of the external and induced parts of RC index
    - RC index is separated into external and induced parts using a prior mantle conductivity model and EM induction equations
    - Less parameters are needed (in CHAOS-7, magnetosphere/total = 613/31757 ≈2%)

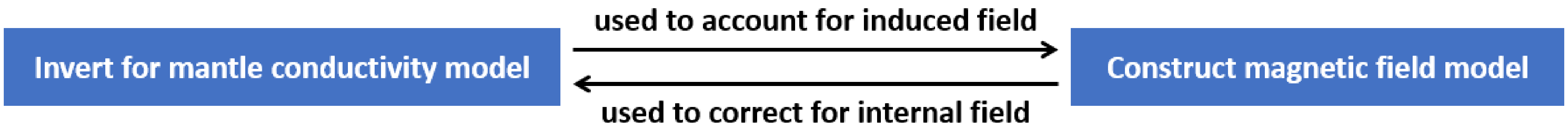

Our approach - incorporating Earth's mantle conductivity during geomagnetic field modeling

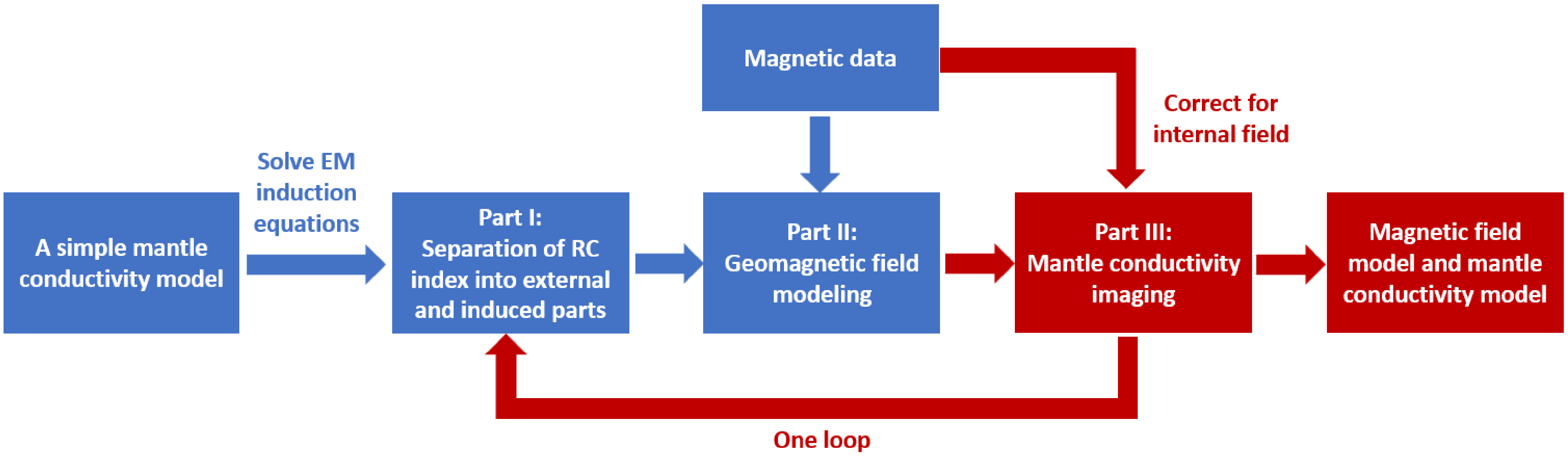

Advantages:

- Constrain geomagnetic field modeling with equation of physics
- Treat geomagnetic field modeling and mantle conductivity imaging in a more self-consistent manner

Method – Part I: separation of RC index into external and induced parts

- Given a mantle conductivity model σ, compute EM responses $Q_1(\omega,\sigma)$ by solving Maxwell's equations using a finite-element code (Yao et al., 2022).

- Separate the RC index into external and internal parts using computed EM responses (Maus and Weidelt, 2004; Olsen et al., 2005)

$$RC(t) = Est(t) + Ist(t,\sigma) = Est(t) + Q_1(t,\sigma) * Est(t)$$

- The time variation of magnetospheric primary and induced fields are expressed by a linear function of the external Est and induced Ist parts of RC index (Olsen et al., 2005).

Method – Part I: separation of RC index into external and induced parts

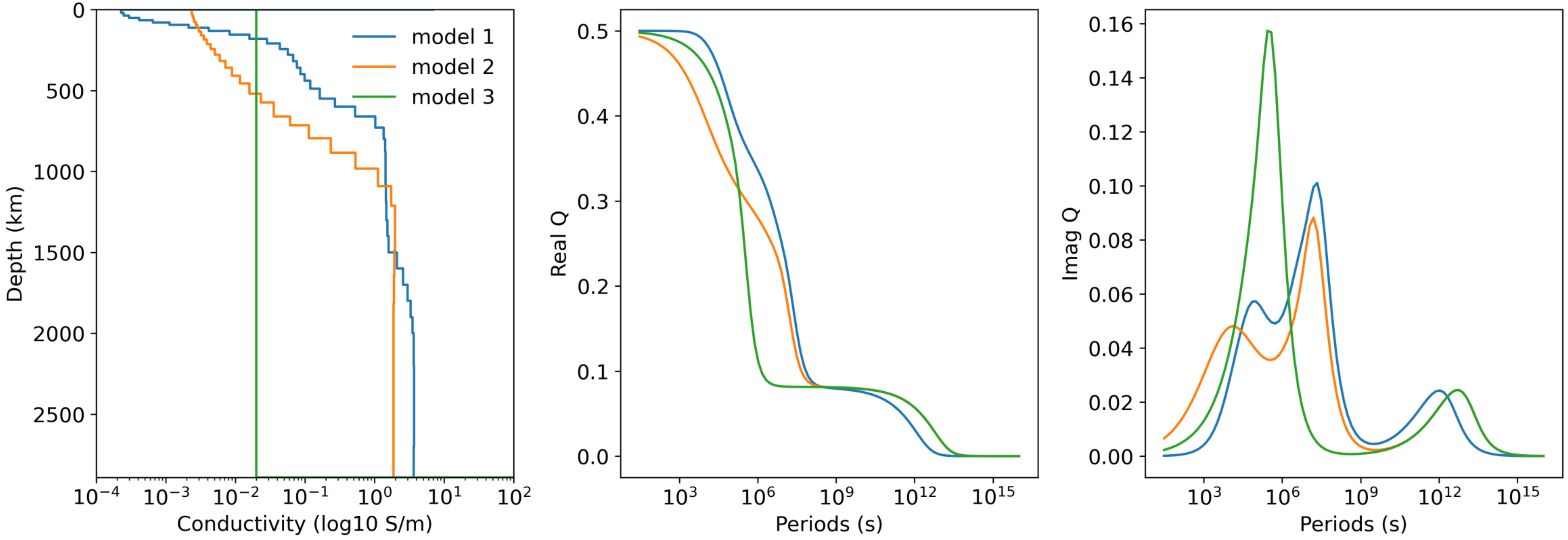

Illustration of EM responses for different Earth's conductivity models
(model 1: Grayver et al., 2017; model 2: Yao et al., 2023a; model 3: half-space model)

Method – Part I: separation of RC index into external and induced parts

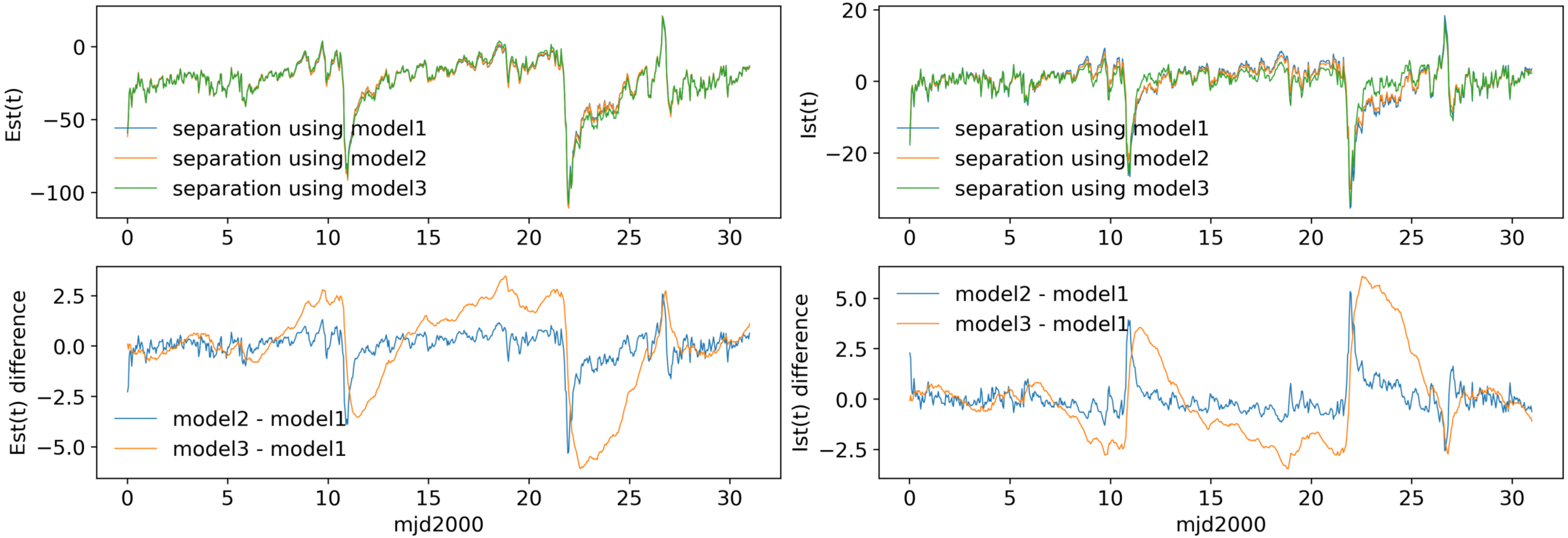

Illustration of RC separation using different Earth's conductivity models

Method – Part II: CHAOS-like geomagnetic field modeling

- **Model parametrization:** core + lithosphere + magnetosphere (Olsen et al., 2006):

$$\mathbf{B} = -\nabla V, V = V^{\text{int}} + V^{ext}$$

$$V^{\text{int}} = a\sum_{n=1}^{N_{\text{int}}}\sum_{m=0}^{n}(g_n^m(t)\cos m\phi + h_n^m(t)\sin m\phi)\left(\frac{a}{r}\right)^{n+1} P_n^m(\cos\theta)$$

$$V^{\text{ext}} = a\sum_{n=1}^{2}\sum_{m=0}^{n}(q_n^{m,SM}(t)\cos m\phi_{SM} + s_n^{m,SM}(t)\sin m\phi_{SM})\left(\frac{r}{a}\right)^{n} P_n^m(\cos\theta_{SM}) + a\sum_{n=1}^{2} q_n^{0,GSM}\left(\frac{r}{a}\right)^{n} P_n^0(\cos\theta_{GSM})$$

- **Model estimation:** we implemented a robust least squares method with Gauss-Newton iteration to minimize the objective function, which includes a data misfit term and two regularization terms (Olsen et al., 2014).

Method – Part II: CHAOS-like geomagnetic field modeling

Validation- reproducing CHAOS-4 model using a new Python code

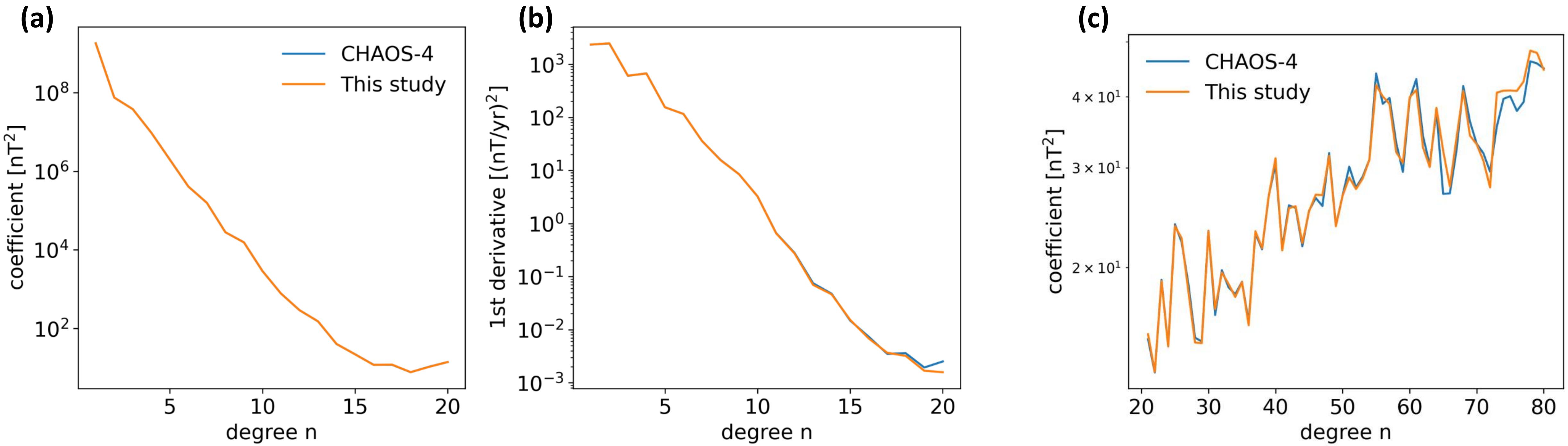

Mauersberger-Lowes spectrum of the (a) core field; (b) secular variation; and (c) lithospheric field of the CHAOS-4 model (Olsen et al., 2014) and the model derived with our code

Method – Part III: mantle conductivity imaging

- Correct for the internal field using the derived geomagnetic field model.
- Invert/update for mantle conductivity model using a trans-dimensional Bayesian inversion code (Yao et al., 2023b).
- Update the magnetic field model using the updated mantle conductivity

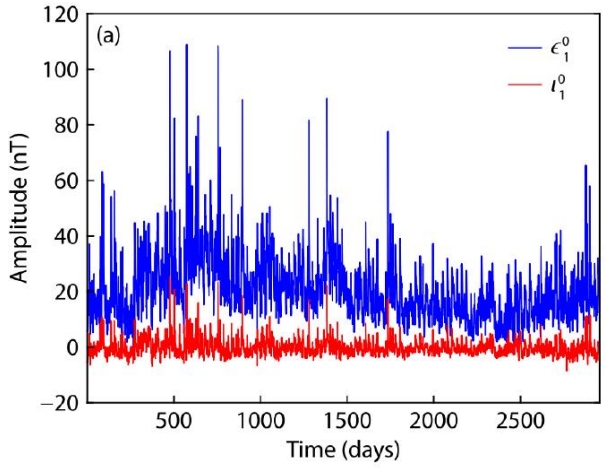

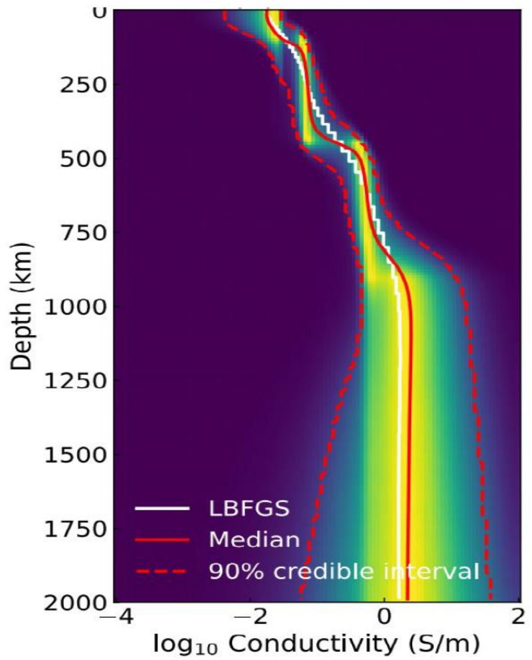

Examples of extracted magnetospheric SH coefficients and recovered mantle conductivity model

Initial results from Swarm and MSS-1 magnetic data

- **Data**
  - Swarm (2023.01-12) and MSS-1 (2023.05-12, launched on May 21, 2023) vector and scalar magnetic data.
  - Only night-time data from geomagnetically quiet times were used
  - 18505 scalar data and 80140 vector data

- **Modeling parameters:**
  - A half-space conductivity model (0.2 S/m) was used for the initial RC separation.
  - Internal fields were estimated up to degree n=30 (n=1-15 is time varying)
  - 1835 model parameters (internal + external + induced)
  - Loop convergence condition: the root-mean-square (rms) error of the magnetic field modeling between adjacent loops is less than 10^{-2}.

Magnetic data residuals

The iteration converges after 3 loops, here are the magnetic field residuals at the last loop:

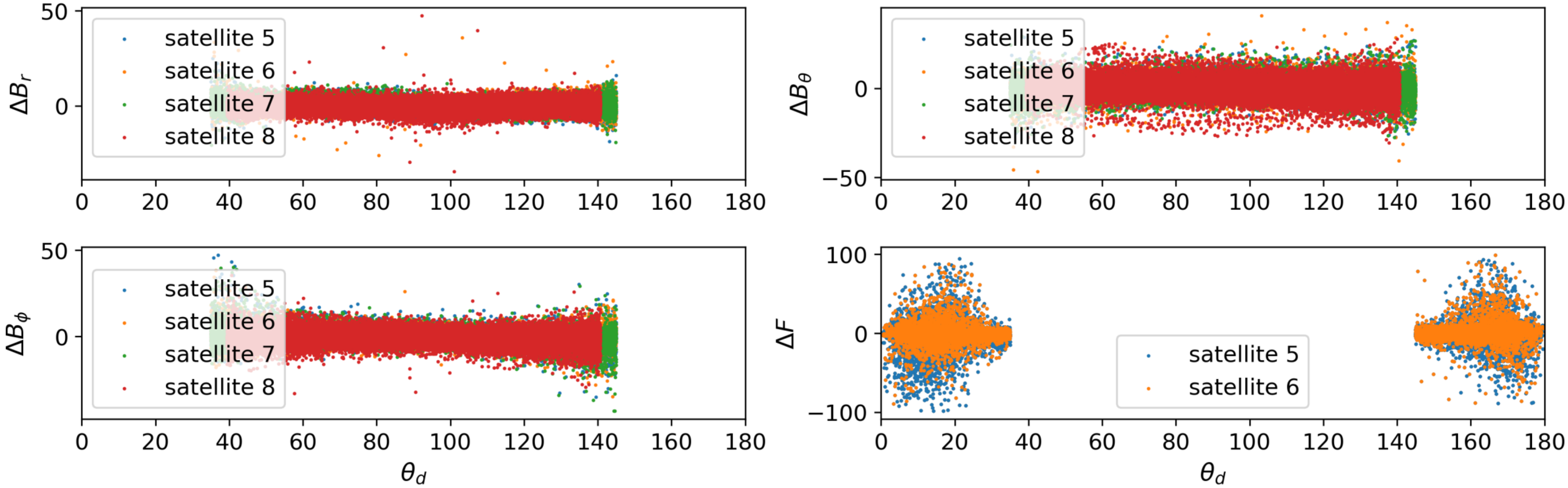

Magnetic data residuals of geomagnetic field modeling at the last loop
(satellite 5-8 denote Swarm A, B, C, and MSS-1, the final Huber-weighted rms is 3.6)

Internal field for different loops

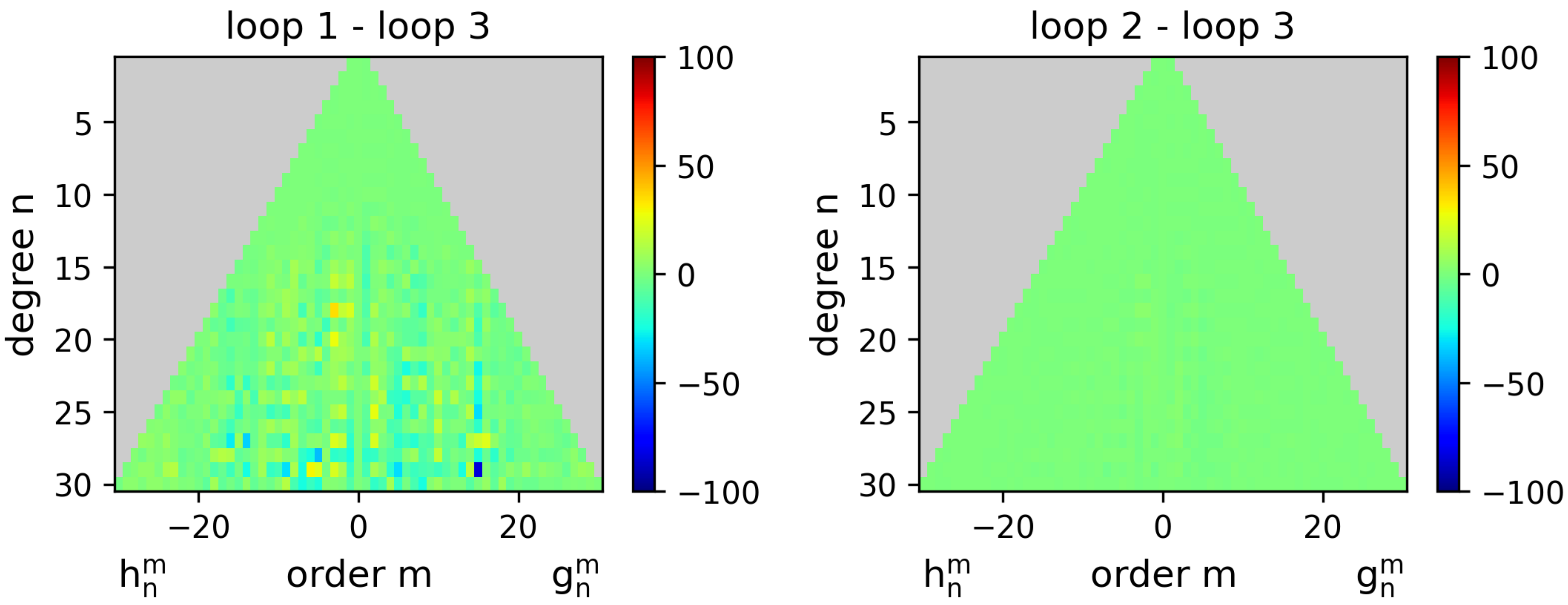

Relative differences of the estimated internal field coefficients between different loops

Internal field for different loops

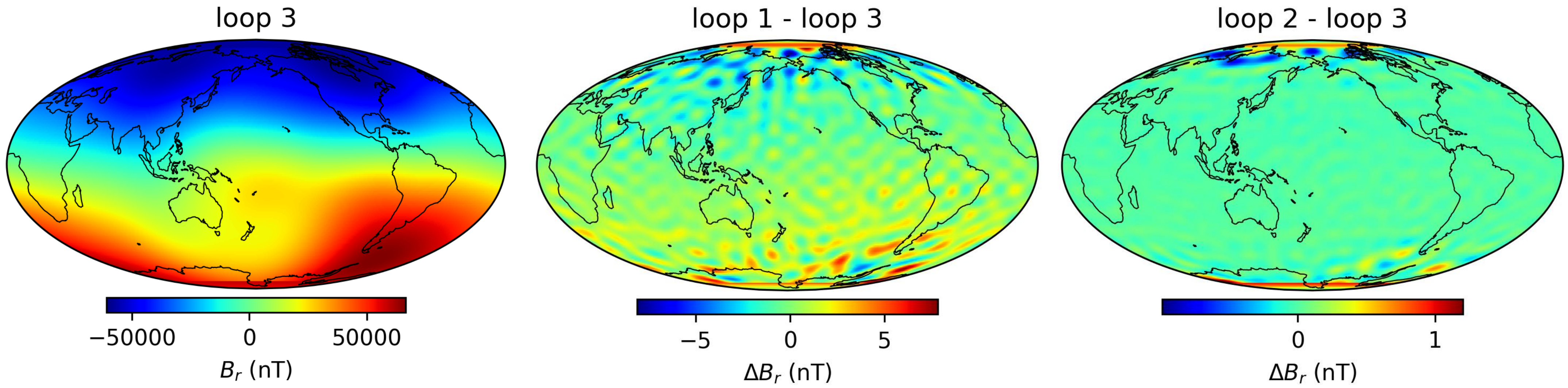

Global maps of internal field (n=1-30, epoch=2023.75) at the Earth's surface and the corresponding differences between different loops

External field for different loops

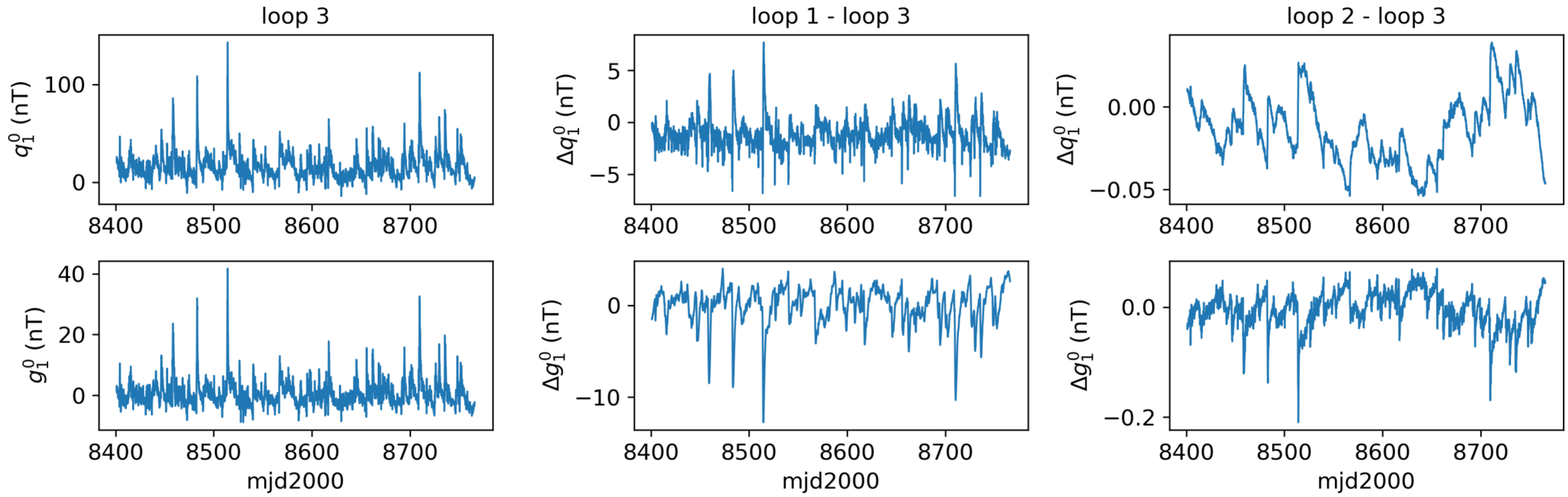

Time series of external and induced coefficients describing large-scale magnetospheric ring current and the corresponding differences between different loops

Mantle conductivity models for different loops

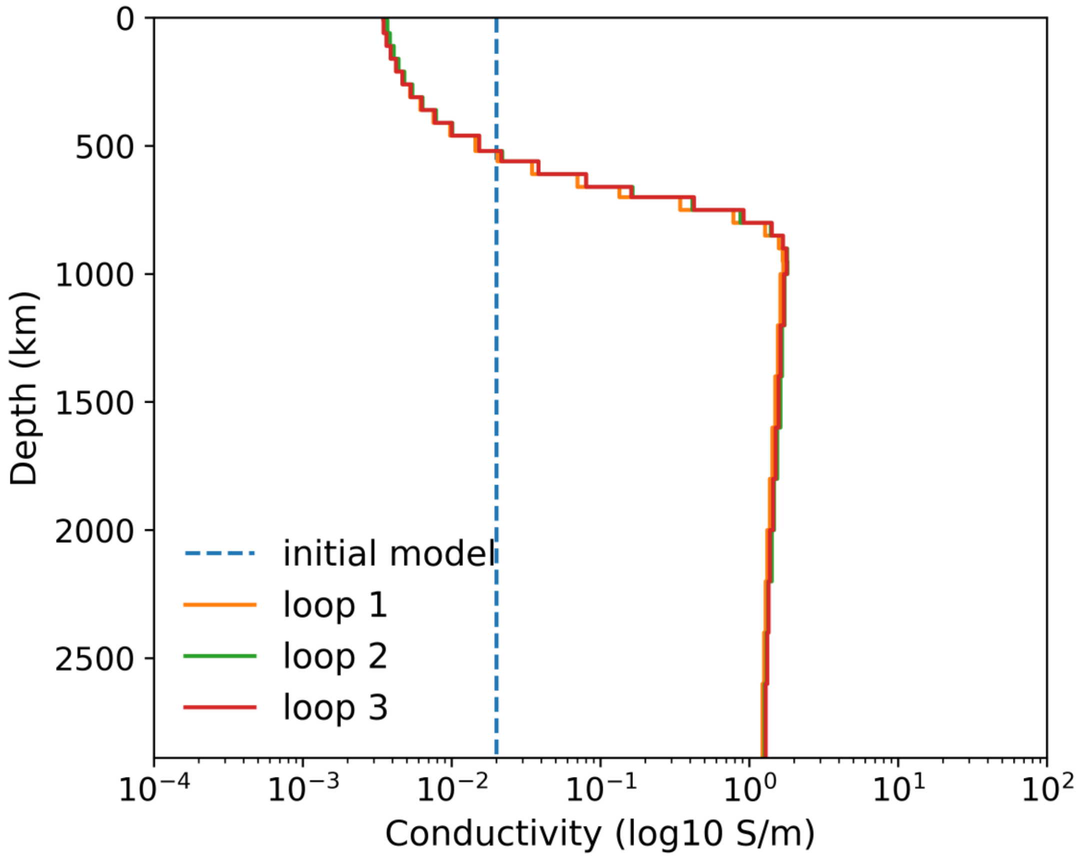

Initial conductivity model used for RC external and induced separation and the recovered mantle conductivity profiles for different loops

Conclusions

- We presented a new method for geomagnetic field modeling that incorporates Earth's mantle conductivity as model parameter.

- Initial results show that inappropriate treatment of induced field may cause error more than 5 nT in both internal and external field models, while our method can iteratively reduce these errors.

- This method may be extended to incorporate more physical processes into geomagnetic field modeling, such as the large-scale ocean circulation and tidal flows.

References

Finlay, C. C., Kloss, C., Olsen, N., Hammer, M. D., Tøffner-Clausen, L., Grayver, A., & Kuvshinov, A. (2020). The CHAOS-7 geomagnetic field model and observed changes in the South Atlantic Anomaly. *Earth, Planets and Space*, *72*(1), 156.

Grayver, A. V., Munch, F. D., Kuvshinov, A. V., Khan, A., Sabaka, T. J., & Tøffner-Clausen, L. (2017). Joint inversion of satellite-detected tidal and magnetospheric signals constrains electrical conductivity and water content of the upper mantle and transition zone. Geophysical Research Letters, 44(12), 6074–6081. https://doi.org/10.1002/2017GL073446

Maus, S., & Weidelt, P. (2004). Separating the magnetospheric disturbance magnetic field into external and transient internal contributions using a 1D conductivity model of the Earth. *Geophysical Research Letters*, *31*(12), L12614.

Olsen, N., & Stolle, C. (2012). Satellite Geomagnetism. *Annual Review of Earth and Planetary Sciences*, *40*(1), 441–465.

Olsen, N., Sabaka, T. J., & Lowes, F. (2005). New parameterization of external and induced fields in geomagnetic field modeling, and a candidate model for IGRF 2005. *Earth, Planets and Space*, *57*(12), 1141–1149.

Olsen, N. (2002). A model of the geomagnetic field and its secular variation for epoch 2000 estimated from Ørsted data. *Geophysical Journal International*, *149*(2), 454–462.

Olsen, N., Lühr, H., Finlay, C. C., Sabaka, T. J., Michaelis, I., Rauberg, J., & Tøffner-clausen, L. (2014). The CHAOS-4 geomagnetic field model. *Geophysical Journal International*, *197*(2), 815–827.

Sabaka, T. J., Tøffner-Clausen, L., Olsen, N., & Finlay, C. C. (2020). CM6: a comprehensive geomagnetic field model derived from both CHAMP and Swarm satellite observations. *Earth, Planets and Space*, *72*(1), 80.

Yao, H., Ren, Z., Tang, J., & Zhang, K. (2022). A Multi-Resolution Finite-Element Approach for Global Electromagnetic Induction Modeling With Application to Southeast China Coastal Geomagnetic Observatory Studies. *Journal of Geophysical Research: Solid Earth*, *127*(8), e2022JB024659.

Yao, H., Ren, Z., Pan, K., Tang, J., & Zhang, K. (2023). A global mantle conductivity model derived from 8 years of Swarm satellite magnetic data. *Earth and Planetary Physics*, *7*(1), 49–56.

Yao, H., Ren, Z., Tang, J., Guo, R., & Yan, J. (2023). Trans-dimensional Bayesian joint inversion of magnetotelluric and geomagnetic depth sounding responses to constrain mantle electrical discontinuities. *Geophysical Journal International*, *233*(3), 1821–1846.